Secondary flows and heat transfer in shallow flow around a cylinder: LES, PIV

Egor Palkin[1,2], *Maxim* Shestakov[1,2], and *Rustam* Mullyadzhanov[1,2]

[1]Institute of Thermophysics SB RAS, 630090, Novosibirsk, Russia
[2]Novosibirsk State University, 630090 , Novosibirsk, Russia

Abstract. We report on Large-eddy simulations (LES) of flow around a short cylinder mounted in a narrow plane channel in a range of Reynolds numbers 1000, 2000, 3750 based on the bulk velocity of the flow and diameter of the cylinder supplemented with Particle image velocimetry (PIV) measurements for the highest considered *Re*. First two cases appear to be steady, however, for *Re*=3750 the flow becomes unsteady with the wake dominated by periodic vortex shedding. In front of the cylinder typical horseshoe vortices are identified intensifying the skin friction and heat transfer on the wall, while in the near wake we observe a quasi-periodic low-frequency secondary motion in the form of a pair of counter-rotating eddies developing in the transverse direction. The Karman vortex street remains the dominant pattern, but further downstream from the cylinder the transport across the channel is associated with the secondary streamwise vortices, as also previously observed in slot jets. We observe their impact on heat transfer and skin friction on the wall of the channel.

1 Introduction

Flows over obstacles in a duct are encountered in a large range of Reynolds number in various engineering applications such as cooling systems, bridge piers, heat exchangers, building sections, junctions in wing-body and turbine blade-rotor systems, among other flows of practical relevance. In such configurations due to adverse pressure gradient strong secondary flows known as horseshoe vortices develop in front of the bluff body increasing local shear stress and heat transfer. Behind the body quasi-periodic vortex shedding results in an unsteady recirculating zone and can initiate the Kármán vortex street with energetic transverse fluctuations. The recirculating bubble is known to exhibit low-frequency motion resulting in the fluctuation of the recirculation zone length [1, 2]. Narrow walls bring additional constrain and complicate the dynamics behind the body [3]. Moreover, the interaction of the Kármán vortex street and walls produce additional streamwise vortices further downstream from the cylinder which were also previously detected in slot jets [4, 5] In this paper we study the effect of various secondary currents and vortical structures in front of the cylinder as well as in the near and far wake further downstream on heat transfer using numerical simulations validated against experiments.

2 Computational details

We used unstructured finite-volume computational code T-Flows [6] with the cell-centered collocated grid structure to solve the spatially filtered Navier-Stokes equations for incompressible fluid and a transport equation for the temperature field acting as a passive scalar with Large-eddy simulation approach [7, 8]. The code features second order accuracy discretization in space and time. The pressure and velocity field are coupled with the SIMPLE algorithm. In the accompanying experiments we used water as the working fluid at a room temperature, thus, Pr=6.13 for all simulations, while Pr_t is assumed to be constant (=0.9). Note that the non-dimensional heat flux vector is $q_i=-(\partial T/\partial x_i)/(\mathrm{RePr})$.

The computational domain is shown at Fig. 1a and it represents a box with dimensions $29D\times20D\times H$ in $x\times y\times z$ (streamwise, spanwise and wall-normal direction), where a circular cylinder of diameter D was placed $14D$ from the inlet boundary (x=0, y=0) and fixed between two parallel plane surfaces at z=0 and $z=H$. The ratio between the cylinder diameter and narrow walls distance is D/H=2.5. No-slip boundary conditions were set at all walls, i.e. z=0 and $z=H$ as well as for side boundaries with $y=-10D$ and $y=10D$ and the surface of the cylinder. We imposed laminar steady parabolic velocity profile and linear in z temperature distribution at the inlet ($x=-14D$), while the convective outflow condition was set at the outlet ($x = 15D$). The non-dimensional temperature on the surface of the cylinder is also set to be linear, varying from the hot to cold wall as $T(z)=1-z/H$. A computational mesh consisted of 16.6×10^6 hexahedral cells for all Re, resulting in following near-wall resolution criteria for Re=3750: $\Delta r^+<0.3$, $(R\Delta\varphi)^+<2.3$ and $\Delta z^+<2.4$, where $R=D/2$.

The experiments were performed with the flow of water in a slot channel with the length and width of $39D$ and $20D$, respectively, where D = 10 mm. In order to provide steady velocity distribution close to parabolic at the inlet, the flow passed through a set of two honeycombs. Velocity fields were measured using Particle Image Velocimetry (PIV) technique. The system consisted of a digital PCO camera (1024 × 1280 pix, 500 Hz) and dual cavity Nd:YAG laser (1000 Hz max. rate, 10 mJ max. energy pulse), which was located perpendicular to the main channel. The thickness of the laser sheet was equal to 0.7 mm. The PIV measurements were performed in a $2D\times2D$ region behind the cylinder. The averaged characteristics were calculated using 1000 instantaneous velocity fields. The spatial resolution was estimated to be 0.3 mm.

3 Results

Figure 1 visualizes vortical structures for all cases considered, it can be seen that for Re=1000 and 2000 the flow is absolutely steady while for Re=3750 the flow becomes unstable featuring quasi-periodic vortex shedding. It can also be demonstrated for the region prior to the cylinder where a horseshoe vortex develops further interacting with a separated shear layer downstream. So far we are not able to answer the question if the instability comes from the wake or from the region in front of the cylinder.

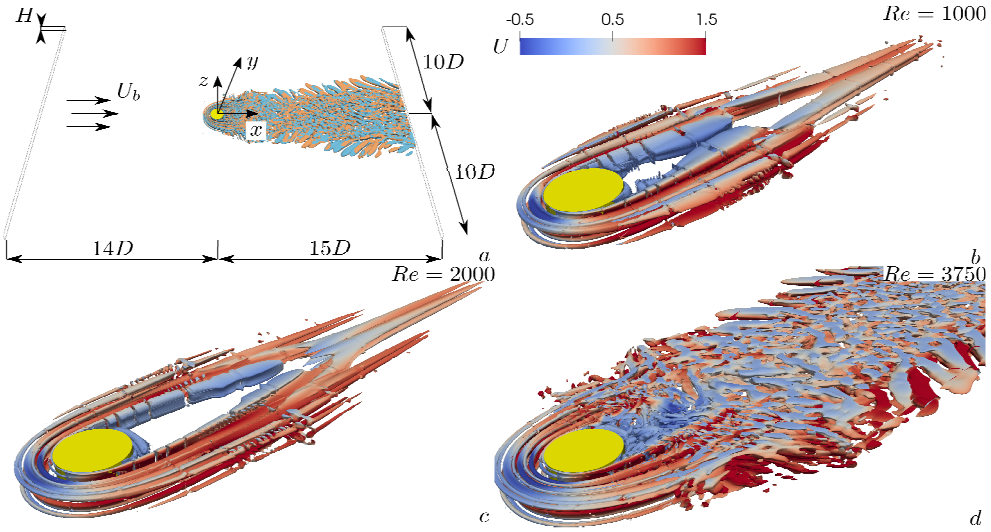

Fig. 2. The scheme of the numerical domain (a) and the instantaneous Q-criterion isosurface for Re=1000(b), Re=2000(c) and Re=3750(d) coloured with the streamwise velocity U from LES.

A snapshot of the transverse vorticity field for two steady cases and a full cycle of dynamics for the highest Re is shown in Fig. 2. The average period of the "shedding" of horseshoe vortices for Re=3750 is around $1.7D/U_b$ against $1.3D/U_b$ obtained for a similar flow for Re=2.5×10^5 in the open channel for D/H = 10 [9].

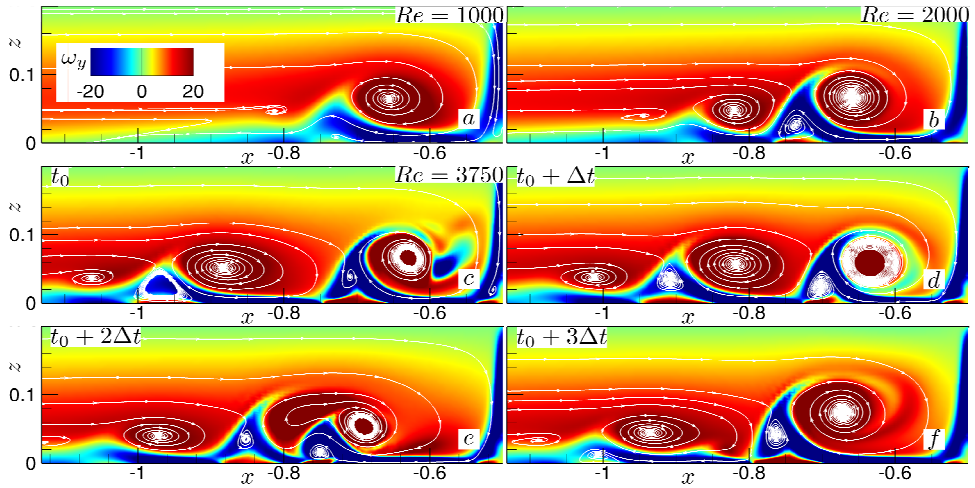

Fig. 2. Instantaneous fields of y vorticity components in x–z plane. (a) Re=1000, (b) Re=2000, (c-f) Re=3750 shown with a time interval $\Delta tU_b/D$=0.4.

As in the case of uniform flow over an infinite cylinder, the steady laminar bubble is longer than its turbulent unsteady counterpart. Right behind the bluff body a static recirculation zone is formed with the length of $L/D \approx 3.2$, 4.1 and 1.2 at Re=1000, 2000 and 3750 correspondingly according to the time-averaged axial velocity field shown on Fig. 3. The length of the recirculating zone is slightly shorter for LES then PIV, while overall results are in satisfactory agreement with experimental measurements. Further downstream an array of streamwise vortices can be clearly seen starting from x/D>0.5 for steady bubble

cases increasing local heat transfer, while on average for turbulent flow case this effect of half-height is less pronounced.

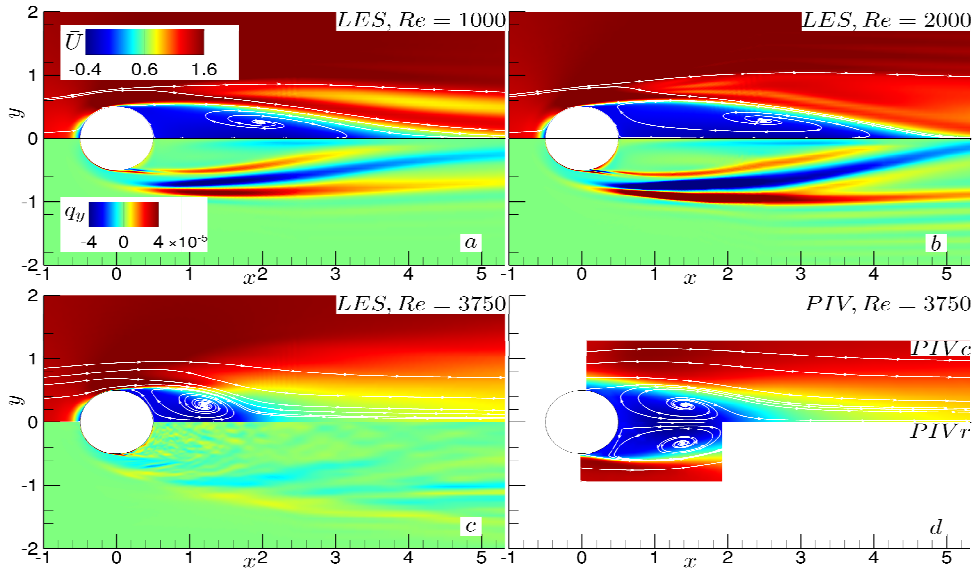

Fig. 3. Time-averaged axial velocity field U/U_b (upper halves) and transverse component q_y of the heat flux vector (lower halves) in the x–z plane in the middle of the channel z/H=0.5 for (a) Re=1000, (b) 2000, (c) 3750 from LES and (d) experiments for Re=3750 and two different spatial resolution levels (PIVc/PIVr standing for coarse and refined resolution).

Mean profiles are presented at Fig. 4 for Re=3750 LES and PIV are considered to be in good agreement. Further downstream an array of streamwise vortices can be clearly seen starting from x/D>0.5 for steady bubble cases increasing local heat transfer, while on average for turbulent flow case this effect of half-height is less pronounced.

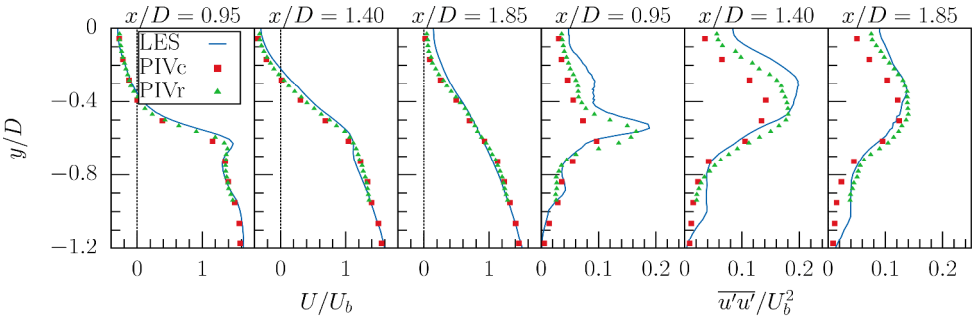

Fig. 4. Time-averaged profiles of axial velocity U/U_b and its fluctuations at several axial stations x/D=0.95, 1.40, 1.85 for Re=3750 from LES (lines) and PIV (symbols).

The streamwise vortical structures shown at Fig. 5 formed in the mixing layers due to entrainment by the turbulent wake, produce strong signatures on the wall in terms of the heat flux and friction. Although main impact increasing heat transfer comes from streaky longitudinal vortices in viscous sublayer, large-scale streamwise structures previously are also revealed at this height at $|y|/D \approx 1.2$ at x/D=4 to $2<|y|/D<3$ at x/D=13. At Re=1000 and 2000 there were no influence on heatflux detected, it is fully homogeneous and U_τ is 2 order of magnitude lower. Their influence on vertical heatfux magnitude was estimated as up to ≈4 times intensification.

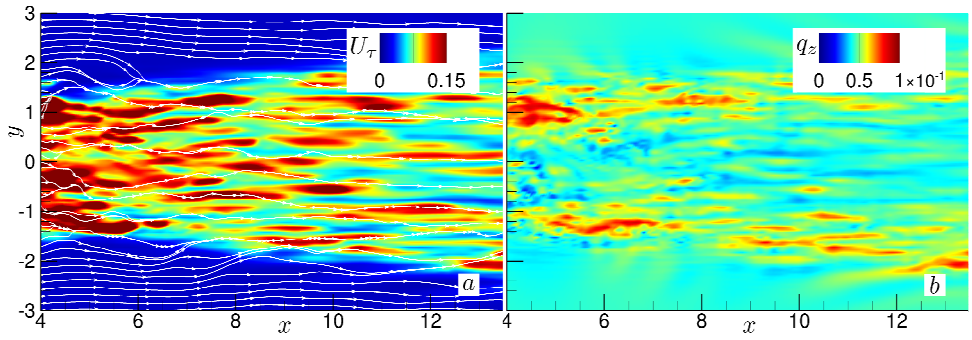

Fig. 5. Instantaneous fields of U_τ/U_b (left) with streamlines and q_z (right) as in on the lower wall (z=0) in x/D and y/D coordinates.

4 Conclusion

We conducted LES simulations at Re=1000, 2000 and 3750 and verified results with against PIV data. With increasing Re magnitude of vertical heat transfer vector component significantly increases in near wake field. At Re=3750 in far wake streamwise vortical structures were identified and effect on heat transfer was estimated in subviscous turbulent flow layer, though no influence were found for Re = 1000 and 2000.

This work is funded by the Russian Foundation For Basic Research grant No. 18-38-00943 and by the Federal Agency for Scientific Organizations (FASO of Russia) Project III.22.7. The computational resources are provided by Siberian Supercomputer Center SB RAS, Joint SuperComputer Center of the Russian Academy of Sciences and Supercomputing Center of the Novosibirsk State University.

References

1. O. Lehmkuhl, I. Rodríguez, R. Borrell, A. Oliva, Phys. Fluids, **25**(8):085109 (2013)
2. E. Palkin, R. Mullyadzhanov, M. Hadžiabdić, K. Hanjalić, Flow Turbul. Combust., **97**(4):1017–1046 (2016)
3. B. Sahin, N.A. Ozturk, C. Gurlek, Int. J Heat and Fluid Flow, **29**:340-351 (2008)
4. M. Shestakov, R. Mullyadzhanov, M. Tokarev, D. Markovich, J. Engineer. Thermophys., **25**(2):159–165 (2016)
5. R. Mullyadzhanov, B. Ilyushin, K. Hanjalić, Int. J. of Heat and Fluid Flow, **56**:284-289 (2015)
6. B. Ničeno, K. Hanjalić, Modelling and Simulation of Turbulent Heat Transfer, 32-73 (2005)
7. D. K. Lilly, Fluid Dyn., **4**(3):633–635 (1992).
8. E. Palkin, M. Hadžiabdić, R. Mullyadzhanov, K. Hanjalić. J. Fluid Mech. **855**: 236-266 (2018)
9. J. Zeng and G. Constantinescu, Phys. Fluids, **29**:066601 (2017)